Psychological stress disturbs bone metabolism via miR-335-3p/Fos signaling in osteoclast

Jiayao Zhang[1], Juan Li[1], Jiehong Huang[2], Xuerui Xiang[2], Ruoyu Li[2], Yun Zhai[1], Shuxian Lin[1#], Weicai Liu[1#]

1 Department of Prosthodontics, Stomatological Hospital and Dental School of Tongji University, Shanghai Engineering Research Center of Tooth Restoration and Regeneration, Shanghai, China.
2 Department of Neurology and Neurological Rehabilitation, Shanghai Yangzhi Rehabilitation Hospital, School of Medicine, Tongji University, Shanghai, China

#Contributed equally

Impact statement

miR-335-3p, which targets FOS and inhibits its activation of NFATC1 signaling, is an important regulator for osteoclast function and responsible for the psychological stress induced osteoporosis

Abstract

It has been well-validated that chronic psychological stress leads to bone loss, but the underlying mechanism remains unclarified. In this study, we established and analyzed the chronic unpredictable mild stress (CUMS) mice to investigate the miRNA-related pathogenic mechanism involved in psychological stress-induced osteoporosis. Our result found that these CUMS mice exhibited osteoporosis phenotype that mainly attributed to the abnormal activities of osteoclasts. Subsequently, miRNA sequencing and other analysis showed that miR-335-3p, which is normally highly expressed in the brain, was significantly down-regulated in the nucleus ambiguous (NAC), serum, and bone of the CUMS mice. Additionally, *in vitro* studies detected that miR-335-3p is important for osteoclast differentiation, with its direct targeting site in Fos. Further studies demonstrated Fos was upregulated in CUMS osteoclast, and the inhibition of Fos suppressed the accelerated osteoclastic differentiation, as well as the expression of osteoclastic genes, such as Nfatc1, Acp5, Mmp9, in miR-335-3p restrained osteoclasts. In conclusion, this work indicated that psychological stress may down-regulate the miR-335-3p expression, which resulted in the accumulation of Fos and the up-regulation of NFACT1 signaling pathway in osteoclasts, leading to its accelerated differentiation and abnormal activity. These results decipher a previously unrecognized paradigm that miRNA can act as a link between psychological stress and bone metabolism.

1 Introduction

Nowadays, chronic psychological stress, a critical public health issue, is getting more and more attention. It is responsible for various systemic diseases, one of which is the

disruption of bone metabolism. Several studies had shown that chronic stress and even depression can lead to osteoporosis(Calarge et al., 2014; Furlan et al., 2005; Yirmiya et al., 2006). Whereas, how does psychological stress signal the brain but affect peripheral organs? Former research suggested that psychological stress can stimulate the autonomic nerves or the central nervous system to disrupt the activation of sympathetic nerves(Kondo & Togari, 2003; Ma et al., 2023) and the endocrine homeostasis(Raison & Miller, 2003) respectively. They alters the levels of neurotransmitters(Chen & Wang, 2017; Foertsch et al., 2017; Guo et al., 2023; Khosla et al., 2018; Teong et al., 2017), neuropeptides(Baldock et al., 2014; Ng & Chin, 2021), hormones(Hasan et al., 2012; Henneicke et al., 2017), related biomolecules, and their corresponding receptors *in vivo*, so as to affect the activations of several signaling pathways. Therefore, it contributes to the increased osteoclast activity, decreased osteoblast activity, and promoted bone matrix degradation, ultimately leading to bone loss. However, treatment of antidepressant and molecules targeting the above-mentioned receptors can only partially alleviate the bone loss(Lam et al., 2022; Marenzana et al., 2007), which suggest that there may be other unanticipated molecular mechanisms involved in psychological stress-induced osteoporosis and efficient for the clinical treatment. Besides, these mentioned neurotransmitters or hormones and their related receptors have broad biological effects, and their effects *in vivo* are highly dose-dependent, which usually give rise to an unpredictable side-effect when using hormonotherapy or neuropeptide therapy for the patients with psychological stress-related osteoporosis(S. Kim et al., 2021; Marenzana et al., 2007; Teong et al., 2017). Therefore, it is full of necessity to further explore alternative mechanisms that implicated in psychological stress-related osteoporosis, since any of these new discoveries will be possible for attracting an ideal clinical therapy with higher biosafety and efficiency.

MicroRNAs (miRNAs) carried by extracellular vesicles (EVs) or proteins *in vivo* are highly involved in biocommunication between multiple organs. They usually have a high regulatory efficiency for targeting multiple transcripts, and a wide regulatory range for controlling the expression of genes coding for protein. Particularly, due to the protection of EVs, they are not only stable in the extracellular environment, such as blood(Chen et al., 2008), but also free to pass through the blood-brain barrier, indicating that miRNAs may work as the linkers between brain and bone. Consistently, a previous study reported that miR-483-5p, stored in brain-derived EVs, could promote bone-fat imbalance in Alzheimer's disease(Liu et al., 2023). Take the consideration that several endogenic miRNAs in the brain(Olejniczak et al., 2018) and blood(Makrygianni & Chrousos, 2023) were reported to change their expression levels after chronic psychological stress, it’s deducible that psychological stress may interfere the bone metabolism through brain-derived miRNAs. Therefore, it is significative and valuable to explore the biofunctions of brain-derived miRNAs during the pathogenesis of psychological stress-related osteoporosis, which can also preliminarily discover the roles of brain-derived miRNAs during the central-peripheral linkage. What's more, as miRNAs are ideal targets for precision therapy due to their effective biofunctions, easy synthesis and longer half-life, exploring their regulatory role in the pathogenesis of the psychological

stress-related osteoporosis is crucial for building the theoretical foundation, based on which, a more efficient and much safer clinical treatment can be developed.

In this context, we primarily established the CUMS model mice, characterized its osteoporosis phenotype, and analyzed the activities of osteoblasts and osteoclasts. Subsequently, using high-throughput miRNA-seq analysis of bone, we identified the potential miRNA candidate that is responsible for bone loss under psychological stress, as well as, investigated the molecular mechanism of this miRNA. Our findings show that the abnormal osteoclast activity is much more responsible for the psychological stress induced osteoporosis. Moreover, miR-335-3p, which can inhibit Fos translation and its integration with Nftac1, is significantly reduced under psychological stress and sequentially enhances the activation of Nftac1 signaling pathway, thereby upregulating the osteoclast differentiation and maturation. These results imply that miR-335-3p plays an important role in the communication between central nervous system and peripheral bone tissue, in addition, provide a new perspective on neuroregulatory mechanisms of the brain that participated in bone metabolism when suffering psychological stress.

2 Results

2.1 CUMS induces behavioral and physiological changes

The mental state of mice were examined by body weight, behavioral and serum parameters. It is showed that the CUMS mice had significantly lower body weights (Figure1B) compared to the control group. They had considerably lower distances (Figure 1C) and times (Figure 1D) within the central area of the open field but did not differ from the control group in terms of the total distance moved in the open field (Figure 1E). Besides, the tail-hanging experiment showed that the immobilization time of mice in the CUMS group to give up struggling was significantly increased (Figure 1F). At the same time, they had lower sucrose preference index (Figure 1G). In addition, serum corticosterone (Figure 1H) and norepinephrine (Figure 1I) levels were significantly elevated in CUMS mice. Taken together, these results all indicated that CUMS modeling caused the mice to develop anxiety and depression-like behaviors.

Figure 1. Effect of CUMS on body weight, behavioral performance, and serum metabolism. (A) Schematic of the procedure used to establish a CUMS model in mice. (B) Body weight (n= 9). (C) Distance moved and (D) Time spent in the central area of OFT (n= 9). (E) Total distance moved in OFT (n=9). (F) Immobility in TST (n=9). (G) Sucrose preference index (n=9). (H) Serum corticosterone levels (n=6). (I) Serum norepinephrine levels (n=5). All data are presented as means ± SD; ns, $P > 0.05$, *, $P < 0.05$, **, $P < 0.01$, ***, $P < 0.001$, by unpaired Student's t-test.

2.2 CUMS leads to bone loss

Next, mouse femurs from different groups were dissected for micro-CT scanning (Figure 2A-D) and H&E staining (Figure 2E). Then quantitatively analyzed histomorphometry, bone mineral density, and bone microarchitecture to assess the bone remodeling

influenced by the psychological stress. It was found that the femurs of CUMS mice had sparse cancellous bone and thinner cortical bone compared to control mice, indicating that psychological stress harmed both cancellous and cortical bone.

Figure 2. Bone mass of the femur decreased in CUMS model. (A) Three-dimensional reconstruction images of femurs from control and CUMS mice. (B) Representative X-ray images of femurs from control and CUMS mice. Quantitative micro-CT analysis of femur (C) trabecular bone and (D) cortical bone. (E)H&E staining. All data are presented as mean ± SD, n=7; *, $P < 0.05$, **, $P < 0.01$, ***, $P < 0.001$, by unpaired Student's t-test.

2.3 CUMS promotes bone formation slightly but enhance osteoclast activity significantly

To further explore the cause of psychological stress induced bone loss, the osteogenic activity of mice were then examined in the CUMS group. Firstly, Masson staining visualized that more osteoid was present in cortical and cancellous bone in CUMS mice (Figure 3A). In addition, the distance between two fluorochromes calcein lines was found wider in CUMS mice, suggesting the mineral deposition rate in CUMS mice was faster than control ones (Figure 3D).Then RNA were isolated to examine osteoblast-related genes, and found that the expression of Osterix (*Osx*), Osteocalcin (*Ocn*), osteopontin (*Opn*), and dentin matrix protein 1 (*Dmp1*) were elevated at the mRNA level in CUMS mice, whereas no significant difference was observed in runt-related transcription factor 2 (*Runx2*) and alkaline phosphatase (*Alp*) (Figure 3E). Further, immunohistochemical staining of OSX and OCN displayed that the protein expression of OSX was higher in CUMS mice (Figure 3B), but no considerable difference could be found in OCN (Figure 3C). Taken together, these data suggested that psychological stress promoted osteoblast functions in CUMS mice.

Since the enhanced osteogenesis could not explain the reduced bone mass under psychological stress, we further examined the osteoclastic activity of CUMS mice. Tartrate-resistant acid phosphatase (TRAP) staining showed a significant increase in the number and area of TRAP-positive osteoclasts under CUMS (Figure 3G-H). Then, RT-PCR analysis of mouse femurs revealed that several osteoclastic genes, such as *Ca2*, *Mmp9*, *Nfatc1*, and *Acp5,* were significantly increased in CUMS mice (Figure 3I, Figure 3— figure supplement 1). Consistently, immunohistochemistry analyses also showed an elevated MMP9 expression in CUMS mice (Figure 3J). Thus, these data demonstrate that osteoclastic activity is elevated *in vivo* under psychological stress, which may be a more direct and vital cause of the decline in bone mass.

Figure 3. Osteogenic and osteoclastic metabolism of mouse femur under psychological stress. (A) Masson staining (B-C) Representative IHC images for OSX, OCN expression in the femur. (D) Calcein double labeling of cortical bone with quantification of MAR (E) qRT-PCR quantification analysis of osteogenic markers including *Osx*, *Ocn*, *Opn*, *Dmp1*, *Runx2*, *Alp*. (F) Representative TRAP staining images of the femur with quantitative

analysis of (G) osteoclast surface per bone surface (Oc.S/BS) and (H) number per bone surface (N.OC/B). (I) qRT-PCR quantification analysis of osteogenic markers including *Ca2*, *Mmp9*, *Nfatc1*, *Acp5*. (J) Representative IHC images for MMP9 in the femur. All data are presented as mean ± SD, n=3; *, P < 0.05, **, P < 0.01, ***, P < 0.001, by unpaired Student's t-test. Scale bar, 100um.

Figure 3— figure supplement 1 qRT-PCR quantification analysis of osteogenic markers including *Oscar*, *Dastamp*, *Calar*, *Ctsk*, *Rank/Opg*, *Clcn7.* All data are presented as mean ± SD, n=3; ns, P > 0.05, by unpaired Student's t-test.

2.4 miR-335-3p is apparently downregulated in CUMS mice

To search the key miRNAs involved in the abnormal bone metabolism correlated to chronic stress, femurs (dissected off the growth plate) were cellected from different groups for sRNA-seq, respectively. The heat map and Volcano plot analysis displayed that a number of miRNAs were significantly altered in CUMS mice (Figure 4A-B). The most significant variations including miR-335-3p, miR-133a-3p, miR-1298-5p, miR-144-5p, miR-1b-5p, mi5-582-3p, based on criteria of |Log2 Fold Change (FC)| > 1.5.

In addition, based on these different expressed miRNAs, miRDB and miRTarBase databases were used to predicted potential target genes, which then performed bioinformatics analysis. In total, 184 GO terms were enriched in target genes according to the criteria FDR < 0.05. The results identified alteration in the DNA binding, transcription activity, cell differentiation, and nervous system development, with most predicted genes being enriched (Figure 4C-D).

miR-335-3p, miR-133a-3p were verified to have significant down-regulation Later, a 3.4-fold and 31-fold decrease in miR-335-3p, miR-133a-3p were further verified by qRT-PCR (Figure 4E). Since upregulation of miR133a has been previously reported to play an important role in postpartum osteoporosis(Li et al., 2018), and is function seems opposite to that in CUMS mice. Together, these results suggest that the decline of miR-335-3p in CUMS mice may be of more concern to us.

In addition, it is stress signals received by the brain that induced local miR-335-3p alterations in bone tissue. miR-335-3p is highly expressed in brain, according to mouse small noncoding RNA tissue atlas (https://www.ccb.uni-saarland.de/asra/) (Figure 4—figure supplement 1). So the expression of miR-335-3p were detected subsequently in five critical brain region, including medial prefrontal cortex (mPFC), NAC, amygdala, hypothalamus, hippocampus, which play key role in receiving and processing chronic stress. Only miR-335-3p was significantly decreased in NAC (Figure 4G). Consistently, the miR-335-3p level in the serum of CUMS mice was also reduced (Figure 4H). These results imply that brain-derived and femur-expressed miR-335-3p maintain bone homeostasis under normal conditions. Psychological stress leads to a decrease in miR-335-3p secreted by NAC, which in turn reduces levels in the femur.

Figure 4. Screening of key miRNAs. (A) The heatmap and (B) Volcano plot for

visualization of differentially expressed miRNAs in the femur proximal to the distal femoral growth plate. ($p < 0.05$) (C-D) Gene Ontology (GO) terms associated with targeted mRNA of differentially expressed miRNAs between groups obtained by database (miRDB and miRTarBase) prediction. (E) Validation by Real-Time expression analysis of miRNAs with statistically significant differences (Con, n=3; CUMS, n=5). (F) Real-Time expression of miR-335-3p in five stress-related brain regions (n=4) and (H) serum (n=3). All data are presented as mean ± SD, n=5; *, $P < 0.05$, **, $P < 0.01$, ***, $P < 0.001$, by unpaired Student's t-test.

Figure 4— figure supplement 1 Reads per million mapped reads (RPMM) expression of miR-335-3p in different tissues.

2.5 miR-335-3p attenuates osteoclast activity

To further confirm whether miR-335-3p affected osteoclast activity, RAW264.7 cells were transfected with mimic-NC, mimic-miR-335-3p, inhibitor-NC or inhibitor-miR-335-3p, respectively (Figure 5—figure supplement 1). Cytochemical TRAP staining showed that mimic-miR-335-3p impaired the activity of osteoclasts, while inhibitor-miR-335-3p significantly promotes the activity of osteoclasts (Figure 5A-D). Next, the mRNA levels of *Acp5*, *Nfatc1*, *and Mmp9* in the indicated RAW264.7 cells were determined by using qRT-PCR. And a significantly decreased expression in these osteoclast-related genes was observed in the mimic-miR-335-3p group, but an increased expression happened in the inhibitor-miR-335-3p group (Figure 5F). Additionally, in the inhibitor-miR-335-3p group, more intranuclear NFATC1, FOS and co-localization signals were observed by immunofluorescence staining, and this response was inhibited by transfection of mimic (Figure 5E).

Figure 5. Initial validation of the function of miR-335-3p. (A) Representative cytochemical TRAP staining images. (B) The amounts of osteoclasts (multinucleated TRAP-positive cells), n=5. (C) The positive TRAP area of osteoclasts, n=5. (D) qRT-PCR quantification analysis of *Acp5*, *Nfatc1*, *Mmp9* expression of RANKL-induced RAW264.7 transfected with mimic-NC, mimic-miR-335-3p, inhibitor-NC, or inhibitor-miR-335-3p, n=3. (E) Representative IF images for FOS, NFATC1, and HOCHEST expression. All data are presented as mean ± SD; *, $P < 0.05$, **, $P < 0.01$, ***, $P < 0.001$, by unpaired Student's t-test. Scale bar, 200um.

Figure 5—supplement 1 Cell transfection efficiency. All data are presented as mean ± SD; *, $P < 0.05$, ****, $P < 0.0001$, by unpaired Student's t-test.

2.6 miR-335-3p alters osteoclast activity by targeting Fos

To seek the downstream molecular mechanisms that mediate the effects of miR-335-3p

on the osteoclast, the ingenuity pathways analysis (IPA) was made based on miR-335-3p and its predicted target gene in miRDB and miRTarBase database. The results show that *Fos*, one of mRNA that miR-335-3p could target with a high prediction score and have a tight connection with osteoclast differentiation and maturation and osteoporosis (Figure 6A). FOS has been previously described as a regulator of transcription factors. It could induce NFATC1 translocation and finally increase the expression of osteogenic markers such as *Acp5*, *Ctsk*, *Mmp9*, and so on(Deng et al., 2022). Kyoto Encyclopedia of Genes and Genomes (KEGG) analysis based on the above predicted target genes resulted in the same higher enrichment for transcription factors activity and DNA binding (Figure 6B).

Next, the dual-luciferase, co-transfection of miR-335-3p, suppressed the luciferase activity of the reporter containing wildtype *Fos* 3'UTR sequence by dual-luciferase reporter assay, which further strongly verifies the direct target relationship between miR-335-3p and *Fos*. But it failed to completely return to normal luciferase activity of two predicted target sites (Figure 6D) deleted construct, which means other binding sites still exist (Figure 6C). Furthermore, at the protein level, there was stronger signals that FOS co-localized with CTSK in the femur of CUMS mice, whose miR-335-3p level decreased (Figure 6E), although no significant difference at mRNA level (Figure 6—figure supplement 1). These results suggest that the enhanced osteoclastic activity under psychological stress may be due to the reduction of miR-335-3p in the femur which in turn slows down its inhibitory effect on Fos in osteoclast.

Moreover, the effect promoting osteoclastic activity of inhibitor-miR-335-3p could be reversed via T-5224, an inhibitor of FOS, measured via TRAP staining and counting (Figure 6F-H). The opposing effects on the mRNA mentioned above levels were also exerted via T-5224 (Figure 6I). These results further demonstrated that miR-335-3p regulates osteoclast activity by targeting Fos.

Figure 6. Seek and verification mechanism of miR-335-3p *in vivo* and *in vitro*.
(A) The IPA analysis of miR-335-3p and its predictive target gene. (B) Kyoto Encyclopedia of Genes and Genomes (KEGG) terms associated with targeted mRNA of differentially expressed miRNAs between groups obtained by database (miRDB and miRTarBase) prediction.(C) Firefly luciferase activity (n=3). (D) Sequence alignment of miR-335-3p and its predictive target sites in 3′UTR of *Fos*. (E) Representative IF images for FOS, CTSK, and HOCHEST expression in the femur (scale bar, 50um). (F) Representative cytochemical TRAP staining images (scale bar, 200um). (G) The amounts and (H) the number of osteoclasts (multinucleated TRAP-positive cells) (n=4). (I) qRT-PCR quantification analysis of *Acp5*, *Nfatc1*, *Mmp9* expression of RANKL-induced RAW264.7 transfected with inhibitor-NC, miR-335-3p-inhibitor, or miR-335-3p-inhibitor+T5224 (n=3) .All data are presented as mean ± SD; *, $P < 0.05$, **, $P < 0.01$, ***, $P < 0.001$, by one-way ANOVA with Tukey's post hoc test.

Figure 6— figure supplement 1 qRT-PCR quantification analysis of *Fos* expression in femur of control and CUMS mice. All data are presented as mean ± SD, n=3; ns, $P > 0.05$,

by unpaired Student's t-test.

Figure7. Schematic model of miR-335-3p as a regulator of osteoclast in psychological stress induced osteoporosis. This study demonstrates that miR-335-3p levels in NAC, serum and bone tissue are decreased under psychological stress, which reduces its targeting of Fos. These promote Fos translation and binding to NFATC1, increasing osteoclast activity and ultimately leading to bone loss.

3 Discussion

Here, we found that psychological stress disturbs bone metabolism *in vivo,* and ultimately leads to bone loss in CUMS mice. We reported for the first time that miR-335-3p could target *Fos* to interfere with its translation and inhibit the activity of NFATC1 signaling pathway, besides, it was significantly reduced in mouse NAC, serum, and bone tissues under psychological stress. Therefore, the osteoclast activity is apparently promoted in CUMS mice, leading to the psychological stress induced osteoporosis. Our study demonstrated that miR-335-3p is a key mediator for nerve-regulated bone metabolism under psychological stress, and it might hold great potential to be a novel therapeutic target.

Previous studies have attributed the psychological stress-induced osteoporosis to the altered neurotransmitters, neuropeptides, and hormones that circulate and localize in tissues via neural and neuroendocrine signaling. In recent years, there has been an increasing focus on the regulatory role of miRNAs in the interaction between organs or systems, since miRNAs that protected by EV can be stably stored and trans, Ported to nearby or even isolated organs and system *in vivo*. Especially their ability to overcome the blood-brain barrier, broaden new horizons for the studies on the interaction between central nervous system and peripheral tissues, for example, bone. Currently, it has been reported that the expression profile of miRNAs was significantly altered in patients with neuropsychiatric disorders(Rao et al., 2013; Wang, 2021; Wu et al., 2022; Żurawek & Turecki, 2021). And some of these miRNAs contained in EVs play a vital role in central regulation in bone metaboliasm. miR-328a-3p and miR-150-5p enriched in EVs from hippocampus after traumatic brain injury accelerate bone healing(Xia et al., 2021). miR-384-5p in brain-derived EVs induces a bone-fat imbalance and bone loss in Alzheimer's disease (Liu et al., 2023). Psychological stress, one of the most common type of neuropsychiatric disorders, is well established as a promoter of osteoporosis, so could miRNAs act as messengers between it and bone homeostasis?

Psychological stress correlated to several brain regions, such as the mPFC, the NAC, the amygdala, the hypothalamus, the hippocampus, etc. Expression levels of several miRNAs related to bone metabolism altered in brain under psychological stress. Hypotheses have been developed on miRNAs that may regulate bone loss under chronic stress(He et al., 2021). However, no study has yet reported whether altered miRNAs in the brain under stress can influence bone metabolism through blood circulation. In this study, for the identification of the key brain region that involved in chronic psychological

stress-related bone metabolism, several miRNAs, which changed their expression levels in the CUMS femur comparing to the control ones, were examined in above mentioned brain regions, such as the mPFC, NAC, amygdala, hypothalamus. It was found that miR-335-3p, which is originally highly expressed in the brain and closely associated with bone metabolism, was significantly down-regulated in the NAC, as well as the serum of CUMS mice. This result is in accordance with the miRNAs sequencing results in the NAC of the CUMS mice reported by Ma K et al(Ma et al., 2019). Taken together, its indicated that the NAC may be one of the important brain regions what is responsible for the psychological stress induced osteoporosis *via* its secretion of miR-335-3p. In another word, these also suggest that the NAC derived and blood-trans, Ported miR-335-3p may have a protective effect on bone homeostasis under normal conditions, while in contrast, chronic stress diminishes the protective effect of miR-335-3p and leads to bone loss.

miR-335-3p is one of the maturation products after shear processing of its precursor mir-335. The other is miR-335-5p, also previously known as miR-335. They may be able to synergistically regulate the progression of diseases (Wilson et al., 2023). Previous psychiatric disease-related studies have mainly focused on miR-335. It play a vital role in the development of depression, both in brain and serum(Bocchio-Chiavetto et al., 2013; Fan et al., 2022; Li et al., 2015; Smalheiser et al., 2012).Therefore, miR-335-3p, which also be present in brain-derived EVs(Tian et al., 2022), could be another significant miRNA involved in psychiatric disorders. At the same time, miR-335-3p also plays a crucial role in the skeletal system. One study reported a significant downregulation of miR-335-3p in the mouse bone tissue of hindlimb unloading osteoporosis model(Huai et al., 2020). Our study further revealed the mechanism of miR-335-3p: It targets *Fos* so as to influence the activity of FOS-NFATC1 signaling pathway. As a result, the down-regulation of miR-335-3p under chronic psychological stress promotes FOS expression and osteoclast activity, leading to osteoporosis.

However, although it’s well verified the consistency of the trend of miR-335-3p in the NAC, serum, and femur, respectively, suggesting miR-335-3p may derived from NAC and targets bone via blood circulation system. Further direct validation is still needed, such as using miRNA tracer mice to demonstrate the importance of brain-derived miRNA. Meanwhile, the potential impact of exogenous miR-335-3p on other bone cells, such as osteoblasts and mesenchymal stem cells, remains to be investigated. Moreover, in addition to the well demonstrated protective effect of miR-335-3p on bone mass *in vitro*, *in vivo* evidences need to be established considering the further therapeutic strategies for psychological stress-induced osteoporosis. Nevertheless, our study confirmed that miR-335-3p may works as a protective effector for bone metabolism during normal conditions and is a key regulator during the pathogenesis of psychological stress-induced osteoporosis.

In conclusion, our study suggests that enhanced osteoclast activity is a major cause of psychological stress-induced osteoporosis. It is found that miR-335-3p regulates osteoclast activity and protects bone metabolic balance by suppressing FOS expression

and FOS-NAFCT1 signaling pathway. However, this protective effect is diminished by chronic psychological stress. These findings provide new insights into the mechanisms of osteoporosis in patients with chronic psychological stress and may aid in the development of new therapeutic strategies.

4 Materials and Methods

4.1 Mice

Male C57BL/6J mice, aged 6 weeks, purchased from Shanghai Model Organisms Center, Inc., were raised at Hubei Laboratory Animal Center, Tongji University, with a 12-hour light/12-hour dark cycle, a room temperature of 22-24 degrees, humidity of 45-55% and free access to food and water. All experimental procedures were approved by and performed in accordance with the standards of the Animal Welfare Committees of Tongji University in Shanghai, China (Number: TJ-HB-LAC-2023-39).

4.2 Establishment of CUMS mouse models

After 1 week of acclimation, 18 mice were divided into the control group and CUMS model Group. CUMS was carried out as described previously(Antoniuk et al., 2019; Willner, 2017) with slight modifications, and the stimulations included 24-hour food deprivation, 24-hour water deprivation, 1 min tail pinch, 7-hour 45° cage tilt, 24-hour wet cage, 5 minutes forced swimming, 5-hour physical restraint, 24-hour day/night reversal. These stressors were randomized to CUMS mice and continued for 6 weeks, while control mice were handled daily in the housing room. Body weight was monitored once every week at 15:30-16:30. Figure 1 A shows the schedule of this study.

4.3 Behavior Analysis

All behavioral tests were done in a dimly lit and quiet room. Animals were acclimatized in the room for at least 2 hours before formal testing. The testing period did not span the diurnal period of the mice. The behavioral performance was monitored and recorded using a digital camera connected to a computer running the Tracking Master software.

4.3.1 Open Field Test (OFT)

The mice were placed in a white open field (40 cm long, 40 cm wide, and 40cm high). The total horizontal distance traveled in 10 minutes, as well as the time and distance traveled in the center area (20 cm* 20 cm) were recorded and calculated. 75% alcohol was used to clean the box during the tests of different mice.

4.3.2 Tail suspension Test (TST)

The mice were suspended individually, with one end of an adhesive tape fixed about 1cm from the tip of the tail, and the other end stocked to the TST apparatus. The mice were held at a 25-30 cm distance between the tip of their nose and the ground. Their behavior was monitored for 6 min, and the immobility time in the latter 4 min was calculated.

4.3.3 Sucrose preference test (SPT)

Mice were single housed and provided with two identical bottles of drinking water. First, Mice were acclimatized to two bottles of normal drinking water for 24 hours. Then, they were given one bottle of normal water and one bottle of 1% sucrose water for the next 24 hours and switched the positions of the two water bottles at the 12th hour. Mice were water and food deprived for 24 hours before the test. During the test, they had free access to normal water and 1% sucrose water, and the positions of the bottles were switched in the middle of the test. The liquid consumption in each bottle over 12 hours was measured, and the sucrose preference index was calculated by dividing the consumption of sucrose solution by the total amount of fluid (water + sucrose).

4.4 Serum Elisa

The concentrations of corticosterone and norepinephrine in serum were measured using elisa kits (Jiangsu MEIMIAN Industrial Co. Ltd., Yancheng, China).

4.5 Micro–CT Analysis

The left femur was dissected from each group of mice, fixed in 4% PFA for 48 hours, and stored in 0.4% PFA until scanning. The femurs were analyzed by micro–CT 50 (Scanco Medical, Zurich, Switzerland) with a scan resolution of a 10-μm slice, a voltage of 70 kV, and a current of 200 μA. To quantify trabecular bone parameters, 60 CT slices immediately proximal to the distal femoral growth plate were analyzed. Bone volume (BV), bone volume over tissue volume (BV/TV), bone mineral density (BMD), trabecular separation (Tb.Sp), trabecular number (Tb.N), trabecular thickness (Tb.Th) were quantified according to the standard procedures.(Y. Kim et al., 2021)

4.6 Histologic Analysis

The right femur samples were fixed with 4% PFA for 48 hours, decalcified in 0.5 mol/L ethylene diamine tetraacetic acid (EDTA, pH 7.4) for 3 weeks, and paraffin-embedded. Next, the samples were sectioned into 4um-thick slices. Hematoxylin & eosin (H&E) (Beyotime, China; C0105S) was conducted to evaluate histological morphology. Osteogenic activities were detected by masson (Servicebio, China; G1006) and immunohistochemical staining for OSX (Abcam, Cambridge, MA, USA; ab22552) and OCN (Affinity, China; DF12303). For double fluorochrome labeling, a total of 2 intraperitoneal injections of calcein (5 mg/kg; Sigma-Aldrich, St. Louis, MO, USA) were given at 7-day intervals at the end of CUMS modeling. Osteoclastic activities were detected by immunohistochemical staining for MMP9 (Abclonal, China; A0289) and TRAP staining (Sigma-Aldrich, St. Louis, MO, USA; 387A). The numbers of osteoclasts (N. OCs/BS/mm) and the TRAP positive surface of osteoclast (OC.S/B) were calculated. At the level of mechanism validation, immunohistochemical staining for FOS (Cell Signaling, USA; #2250), CTSK (Santa Cruz Biotechnology, CA, USA; sc-48353), NFATC1 (Santa Cruz Biotechnology, CA, USA; sc-7294), HOCHEST (ThermoFisher, Waltham, USA; H3570) was used to observe the location and abundance of protein expression

4.7 Quantitative RT-PCR Analysis

Total RNA was extracted from tissues or cells using RNAiso Plus (Takara Biotechnology, Japan; 9109) according to the manufacturer's guidelines. RNA concentration was assessed by NanoDrop One. For mRNAs, cDNA was synthesized using PrimeScript™ RT Master Mix (Takara Biotechnology, Japan; RR036A) , and a reaction mix was prepared using SYBR green master mix (Yeasen, Shanghai, China; 11201ES08). For miRNAs, miDETECT A TrackTM miRNA qRT-PCR Starter Kit (RIBOBIO, Guangzhou, China; C10712-1) was used. The expression levels of the target gene were calculated by the comparative Ct ($2^{-\Delta\Delta CT}$) method using GAPDH or U6 for normalization, respectively, using CFX Opus 96 (Bio-Rad Laboratories, Hercules, CA, USA). The amplifications of the miRNAs were carried out by using miR-335-3p-F, miR-133a-3p-F, miR-1298-5p-F, miR-144-5p-F, miR-1b-5p-F, miR-582-3p-F, miR-141-3p-F, and U6-F as forward primer and unified reverse primer (URP) as a reverse primer to amplify miR-335-3p, miR-133a-3p, miR-193b-3p, miR-1298-5p, miR-144-5p, miR-1b-5p, miR-582-3p, miR-141-3p and U6, respectively. The primer sequences were as follows:

Gene	**5'- 3'**
mouse-OPG-F	ACCCAGAAACTGGTCATCAGC
mouse-OPG-R	CTGCAATACACACACTCATCACT
mouse-RANKL-F	CAGCATCGCTCTGTTCCTGTA
mouse-RANKL-R	CTGCGTTTTCATGGAGTCTCA
mouse-Nfatc1-F	ATGCGAGCCATCATCGA
mouse-Nfatc1-R	GGGATGTGAACTCGGAAGAC
mouse-Acp5-F	GACAAGAGGTTCCAGGAGACC
mouse-Acp5-R	GGGCTGGGGAAGTTCCAG
mouse-Calcr-F	CGTTCTTTATTACCTGGCTCTTGTG
mouse-Calcr-R	TCTGGCAGCTAAGGTTCTTGAAA
mouse-Mmp9-F	GGAACTCACACGACATCTTCCA
mouse-Mmp9-R	GAAACTCACACGCCAGAAGAATTT
mouse-Ca2-F	GCTGCAGAGCTTCACTTGGT
mouse-Ca2-R	AAACAGCCAATCCATCCGGT
mouse-Oscar-F	TGGTCATCAGTTTCGAAGGTTCT
mouse-Oscar-R	CAGCCCCAAACGGATGAG
mouse-Dcstamp-F	TGTATCGGCTCATCTCCTCCAT
mouse-Dcstamp-R	GACTCCTTGGGTTCCTTGCTT
mouse-Clcn7-F	AGCCTGGACTATGACAACAGC
mouse-Clcn7-R	GGAAAGCCGTGTGGTTGATT
mouse-ctsk-F	GAAGCAGTATAACAGCAAGGTGGAT
mouse-ctsk-F	TGTCTCCCAAGTGGTTCATGG
mouse-SP7-F	ATGGCGTCCTCTCTGCTTG
mouse-SP7-R	TGAAAGGTCAGCGTATGGCTT

mouse-OCN-F	CTGACCTCACAGATgCCAAGC
mouse-OCN-R	TGGTCTGATAGCTCGTCACAAG
mouse-OPN-F	AGCAAGAAACTCTTCCAAGCAA
mouse-OPN-R	GTGAGATTCGTCAGATTCATCCG
mouse-dmp1-F	CATTCTCCTTGTGTTCCTTTGGG
mouse-dmp1-R	TGTGGTCACTATTTGCCTGTc
mouse-RUNX2-F	CCTTTACCTACACCCCGCCA
mouse-RUNX2-R	GGATGCTGACGAAGTACCAT
mouse-ALP-F	CCAACTCTTTTGTGCCAGAGA
mouse-ALP-R	GGCTACATTGGTGTTGAGCTTTT
mouse-Gapdh-F	AGGTCGGTGTGAACGGATTTG
mouse-Gapdh-R	GGGGTCGTTGATGGCAACA
mmu-miR-335-3p-F	UUUUUCAUUAUUGCUCCUGACC
mmu-miR-1298-5p-F	UUCAUUCGGCUGUCCAGAUGUA
mmu-miR-144-5p-F	GGAUAUCAUCAUAUACUGUAAGU
mmu-miR-141-3p-F	UAACACUGUCUGGUAAAGAUGG
mmu-miR-133a-3p.1-F	UUGGUCCCCUUCAACCAGCUG
mmu-miR-193b-3p-F	AACUGGCCCACAAAGUCCCGCU
mmu-miR-1b-5p-F	TGGTTTTTGGGGTACATACTTCTTTAC
mmu-miR-582-3p-F	UAACCUGUUGAACAACUGAAC

4.8 microRNA sequencing (sRNA-Seq)

Total RNA was extracted from M-exos and HM-exos using the Trizol reagent (Takara Biotechnology, Japan; 9109), and RNA integrity was assessed using a 2100 bioanalyzer (Agilent Technologies, CA, USA). An Illumina TruSeq Small RNA kit (Illumina, San Diego, CA, USA) was used to construct the library, and a high-throughput sequencing platform was used to sequence the enriched 18–32 nt Small RNA fragments. The differentially expressed miR NAs in the two groups of exosomes were screened (p-value < 0.05), and miRDB (http://www.mirdb.org/) and DIANA (https://dianalab.e-ce.uth.gr/) databases were used to predict the target genes of the miRNAs, and KEGG enrichment analysis was performed for the identified target genes.

4.9 3'UTR luciferase reporter assay

A fragment of the Fos 3′UTR containing wildtype (WT) or mutant (Mut) predicted two binding sites from TargetScan (http://www.targetscan.org) database for miR-335-3p was inserted into the pMIR-REPORT vector. HEK293 cells were cotransfected with either Fos-WT or Fos-Mut vector and either miR-335-3p mimic or miRNA mimic negative control (mimic NC) using Lipofectamine 2000 (Invitrogen, USA; 11668019). Luciferase activity was determined at 48 h post-transfection using the Dual-Glo Luciferase Assay System (Promega, Madison, WI; E2940) following the manufacturer's instructions. Data were normalized by dividing firefly luciferase activity with that of Renilla luciferase enzyme activity.

4.10 Cell culture and transfection

The Raw 264.7 cells (gifts from Dr. Shengbing Yang, Shanghai Key Laboratory of Orthopaedic Implants, Department of Orthopaedic Surgery, Shanghai Ninth People's Hospital, Shanghai Jiao Tong University School of Medicine, Shanghai, 200125, China) were used for osteoclastic differentiation induction via RANKL (R&D Systems, USA; 462-TEC) (50nM). The entire inducing process lasted 4 days , and medium refreshed every three days. In addition, BMSCs were transfected with miR-335-3p mimic, miR-335-3p inhibitor and NC that synthesized by RiboBio (Guangzhou, China) via Fugene HD (Promega, Madison, WI, USA; E2311) when cells confluency reached 50%.

4.11 Statistical analysis

Data are represented as the mean±SD. Differences between 2 groups were determined by Student's t test. Differences among 3 groups were determined by one-way ANOVA with Tukey's post hoc test. All experiments were repeated at least three times. A value of $P < 0.05$ was considered significant.

5 Data availability

All data generated or analysed during this study are included in the manuscript and supporting file.

6 Reference

Antoniuk, S., Bijata, M., Ponimaskin, E., & Wlodarczyk, J. (2019). Chronic unpredictable mild stress for modeling depression in rodents: Meta-analysis of model reliability. *Neuroscience and biobehavioral reviews, 99*, 101-116. https://doi.org/10.1016/j.neubiorev.2018.12.002

Baldock, P. A., Lin, S., Zhang, L., Karl, T., Shi, Y., Driessler, F., Zengin, A., Hörmer, B., Lee, N. J., Wong, I. P., Lin, E. J., Enriquez, R. F., Stehrer, B., During, M. J., Yulyaningsih, E., Zolotukhin, S., Ruohonen, S. T., Savontaus, E., Sainsbury, A., & Herzog, H. (2014, Oct). Neuropeptide y attenuates stress-induced bone loss through suppression of noradrenaline circuits. *J Bone Miner Res, 29*(10), 2238-2249. https://doi.org/10.1002/jbmr.2205

Bocchio-Chiavetto, L., Maffioletti, E., Bettinsoli, P., Giovannini, C., Bignotti, S., Tardito, D., Corrada, D., Milanesi, L., & Gennarelli, M. (2013). Blood microRNA changes in depressed patients during antidepressant treatment. *European Neuropsychopharmacology : the Journal of the European College of Neuropsychopharmacology, 23*(7), 602-611. https://doi.org/10.1016/j.euroneuro.2012.06.013

Calarge, C. A., Butcher, B. D., Burns, T. L., Coryell, W. H., Schlechte, J. A., & Zemel, B. S. (2014, Oct). Major depressive disorder and bone mass in adolescents and young adults. *J Bone Miner Res, 29*(10), 2230-2237. https://doi.org/10.1002/jbmr.2249

Chen, D., & Wang, Z. (2017, Jan). Adrenaline inhibits osteogenesis via repressing miR-21 expression. *Cell Biol Int, 41*(1), 8-15. https://doi.org/10.1002/cbin.10685

Chen, X., Ba, Y., Ma, L., Cai, X., Yin, Y., Wang, K., Guo, J., Zhang, Y., Chen, J., Guo, X., Li, Q., Li, X., Wang, W., Zhang, Y., Wang, J., Jiang, X., Xiang, Y., Xu, C., Zheng, P., Zhang, J., Li, R., Zhang, H., Shang, X., Gong, T., Ning, G., Wang, J., Zen, K., Zhang, J., & Zhang, C.-Y. (2008). Characterization of microRNAs in serum: a novel class of biomarkers for diagnosis of cancer and other diseases. *Cell Research, 18*(10). https://doi.org/10.1038/cr.2008.282

Deng, W., Ding, Z., Wang, Y., Zou, B., Zheng, J., Tan, Y., Yang, Q., Ke, M., Chen, Y., Wang, S., & Li, X. (2022). Dendrobine attenuates osteoclast differentiation through modulating ROS/NFATc1/ MMP9 pathway and prevents inflammatory bone destruction. *Phytomedicine : International Journal of Phytotherapy and Phytopharmacology, 96*, 153838. https://doi.org/10.1016/j.phymed.2021.153838

Fan, C., Li, Y., Lan, T., Wang, W., Long, Y., & Yu, S. Y. (2022). Microglia secrete miR-146a-5p-containing exosomes to regulate neurogenesis in depression. *Molecular Therapy : the Journal of the American Society of Gene Therapy, 30*(3), 1300-1314. https://doi.org/10.1016/j.ymthe.2021.11.006

Foertsch, S., Haffner-Luntzer, M., Kroner, J., Gross, F., Kaiser, K., Erber, M., Reber, S. O., & Ignatius, A. (2017, Dec 19). Chronic psychosocial stress disturbs long-bone growth in adolescent mice. *Dis Model Mech, 10*(12), 1399-1409. https://doi.org/10.1242/dmm.030916

Furlan, P. M., Ten Have, T., Cary, M., Zemel, B., Wehrli, F., Katz, I. R., Gettes, D. R., & Evans, D. L. (2005, Apr 15). The role of stress-induced cortisol in the relationship between depression and decreased bone mineral density. *Biol Psychiatry, 57*(8), 911-917. https://doi.org/10.1016/j.biopsych.2004.12.033

Guo, Q., Chen, N., Qian, C., Qi, C., Noller, K., Wan, M., Liu, X., Zhang, W., Cahan, P., & Cao, X. (2023). Sympathetic Innervation Regulates

Osteocyte-Mediated Cortical Bone Resorption during Lactation. *Advanced Science (Weinheim, Baden-Wurttemberg, Germany)*, e2207602. https://doi.org/10.1002/advs.202207602

Hasan, K. M., Rahman, M. S., Arif, K. M., & Sobhani, M. E. (2012, Dec). Psychological stress and aging: role of glucocorticoids (GCs). *Age (Dordr), 34*(6), 1421-1433. https://doi.org/10.1007/s11357-011-9319-0

He, Y., Wuertz-Kozak, K., Kuehl, L., & Wippert, P. (2021). Extracellular Vesicles: Potential Mediators of Psychosocial Stress Contribution to Osteoporosis? *International journal of molecular sciences, 22*(11). https://doi.org/10.3390/ijms22115846

Henneicke, H., Li, J., Kim, S., Gasparini, S. J., Seibel, M. J., & Zhou, H. (2017). Chronic Mild Stress Causes Bone Loss via an Osteoblast-Specific Glucocorticoid-Dependent Mechanism. *Endocrinology, 158*(6), 1939-1950. https://doi.org/10.1210/en.2016-1658

Huai, Y., Zhang, W., Chen, Z., Zhao, F., Wang, W., Dang, K., Xue, K., Gao, Y., Jiang, S., Miao, Z., Li, M., Hao, Q., Chen, C., & Qian, A. (2020). A Comprehensive Analysis of MicroRNAs in Human Osteoporosis. *Frontiers In Endocrinology, 11*, 516213. https://doi.org/10.3389/fendo.2020.516213

Khosla, S., Drake, M. T., Volkman, T. L., Thicke, B. S., Achenbach, S. J., Atkinson, E. J., Joyner, M. J., Rosen, C. J., Monroe, D. G., & Farr, J. N. (2018). Sympathetic β1-adrenergic signaling contributes to regulation of human bone metabolism. *The Journal of Clinical Investigation, 128*(11), 4832-4842. https://doi.org/10.1172/JCI122151

Kim, S., Henneicke, H., Cavanagh, L. L., Macfarlane, E., Thai, L. J., Foong, D., Gasparini, S. J., Fong-Yee, C., Swarbrick, M. M., Seibel, M. J., & Zhou, H. (2021). Osteoblastic glucocorticoid signaling exacerbates high-fat-diet- induced bone loss and obesity. *Bone Research, 9*(1), 40. https://doi.org/10.1038/s41413-021-00159-9

Kim, Y., Brodt, M. D., Tang, S. Y., & Silva, M. J. (2021). MicroCT for Scanning and Analysis of Mouse Bones. *Methods In Molecular Biology (Clifton, N.J.), 2230*, 169-198. https://doi.org/10.1007/978-1-0716-1028-2_11

Kondo, A., & Togari, A. (2003, Sep). In vivo stimulation of sympathetic nervous system modulates osteoblastic activity in mouse calvaria. *American Journal of Physiology-Endocrinology and Metabolism, 285*(3), E661-E667. https://doi.org/10.1152/ajpendo.00026.2003

Lam, R. W., Wong, H.-K., Kumarsing, R. A., Chua, A. N., Ho, R. C., McIntyre, R. S., & Ho, C. S. (2022). Fluoxetine improves bone microarchitecture and mechanical properties in rodents undergoing chronic mild stress - an animal model of depression. *Translational Psychiatry, 12*(1), 339. https://doi.org/10.1038/s41398-022-02083-w

Li, J., Meng, H., Cao, W., & Qiu, T. (2015). MiR-335 is involved in major depression disorder and antidepressant treatment through targeting GRM4. *Neuroscience Letters, 606*, 167-172. https://doi.org/10.1016/j.neulet.2015.08.038

Li, Z., Zhang, W., & Huang, Y. (2018). MiRNA-133a is involved in the regulation of postmenopausal osteoporosis through promoting osteoclast differentiation. *Acta Biochimica Et Biophysica Sinica, 50*(3), 273-280. https://doi.org/10.1093/abbs/gmy006

Liu, X., Chen, C., Jiang, Y., Wan, M., Jiao, B., Liao, X., Rao, S., Hong, C., Yang, Q., Zhu, Y., Liu, Q., Luo, Z., Duan, R., Wang, Y., Tan, Y., Cao, J., Liu, Z., Wang, Z., Xie, H., & Shen, L. (2023). Brain-derived extracellular vesicles promote bone-fat imbalance in Alzheimer's disease. *International Journal of Biological Sciences, 19*(8), 2409-2427. https://doi.org/10.7150/ijbs.79461

Ma, C., Zhang, Y., Cao, Y., Hu, C.-H., Zheng, C.-X., Jin, Y., & Sui, B.-D. (2023). Autonomic Neural Regulation in Mediating the Brain-Bone Axis: Mechanisms and Implications for Regeneration under Psychological Stress. *QJM : Monthly Journal of the Association of Physicians*. https://doi.org/10.1093/qjmed/hcad108

Ma, K., Zhang, H., Wei, G., Dong, Z., Zhao, H., Han, X., Song, X., Zhang, H., Zong, X., Baloch, Z., & Wang, S. (2019). Identification of key genes, pathways, and miRNA/mRNA regulatory networks of CUMS-induced depression in nucleus accumbens by integrated bioinformatics analysis. *Neuropsychiatric Disease and Treatment, 15*, 685-700. https://doi.org/10.2147/NDT.S200264

Makrygianni, E. A., & Chrousos, G. P. (2023, Feb). Extracellular vesicles and the Stress System. *Neuroendocrinology, 113*(2), 120-167. https://doi.org/10.1159/000527182

Marenzana, M., De Souza, R. L., & Chenu, C. (2007, Aug). Blockade of beta-adrenergic signaling does not influence the bone mechano-adaptive response in mice. *Bone, 41*(2), 206-215.

https://doi.org/10.1016/j.bone.2007.04.184

Ng, J. S., & Chin, K. Y. (2021). Potential mechanisms linking psychological stress to bone health. *Int J Med Sci, 18*(3), 604-614. https://doi.org/10.7150/ijms.50680

Olejniczak, M., Kotowska-Zimmer, A., & Krzyzosiak, W. (2018). Stress-induced changes in miRNA biogenesis and functioning. *Cellular and Molecular Life Sciences : CMLS, 75*(2), 177-191. https://doi.org/10.1007/s00018-017-2591-0

Raison, C. L., & Miller, A. H. (2003, Sep). When Not Enough Is Too Much: The Role of Insufficient Glucocorticoid Signaling in the Pathophysiology of Stress-Related Disorders. *American Journal of Psychiatry, 160*(9), 1554-1565. https://doi.org/10.1176/appi.ajp.160.9.1554

Rao, P., Benito, E., & Fischer, A. (2013). MicroRNAs as biomarkers for CNS disease. *Frontiers In Molecular Neuroscience, 6*, 39. https://doi.org/10.3389/fnmol.2013.00039

Smalheiser, N. R., Lugli, G., Rizavi, H. S., Torvik, V. I., Turecki, G., & Dwivedi, Y. (2012). MicroRNA expression is down-regulated and reorganized in prefrontal cortex of depressed suicide subjects. *PLoS One, 7*(3), e33201. https://doi.org/10.1371/journal.pone.0033201

Teong, B., Kuo, S. M., Tsai, W.-H., Ho, M.-L., Chen, C.-H., & Huang, H. H. (2017). Liposomal Encapsulation for Systemic Delivery of Propranolol via Transdermal Iontophoresis Improves Bone Microarchitecture in Ovariectomized Rats. *International journal of molecular sciences, 18*(4). https://doi.org/10.3390/ijms18040822

Tian, Y., Zhao, R., Li, X., Zhou, J., Zhan, D., Wang, Y., He, Y., Zhang, J., & Yuan, H. (2022). Alterations of microRNAs expression profiles in small extracellular vesicle after traumatic brain injury in mice. *Experimental Animals, 71*(3), 329-337. https://doi.org/10.1538/expanim.21-0148

Wang, H. (2021). MicroRNAs, Multiple Sclerosis, and Depression. *International journal of molecular sciences, 22*(15). https://doi.org/10.3390/ijms22157802

Willner, P. (2017). Reliability of the chronic mild stress model of depression: A user survey. *Neurobiology of stress, 6*, 68-77. https://doi.org/10.1016/j.ynstr.2016.08.001

Wilson, T. G., Baghel, M., Kaur, N., Moutzouros, V., Davis, J., & Ali, S. A. (2023). Characterization of miR-335-5p and miR-335-3p in human osteoarthritic tissues. *Arthritis Research & Therapy, 25*(1), 105. https://doi.org/10.1186/s13075-023-03088-6

Wu, Z., Cai, Z., Shi, H., Huang, X., Cai, M., Yuan, K., Huang, P., Shi, G., Yan, T., & Li, Z. (2022). Effective biomarkers and therapeutic targets of nerve-immunity interaction in the treatment of depression: an integrated investigation of the miRNA-mRNA regulatory networks. *Aging, 14*(8), 3569-3596. https://doi.org/10.18632/aging.204030

Xia, W., Xie, J., Cai, Z., Liu, X., Wen, J., Cui, Z.-K., Zhao, R., Zhou, X., Chen, J., Mao, X., Gu, Z., Zou, Z., Zou, Z., Zhang, Y., Zhao, M., Mac, M., Song, Q., & Bai, X. (2021). Damaged brain accelerates bone healing by releasing small extracellular vesicles that target osteoprogenitors. *Nature communications, 12*(1), 6043. https://doi.org/10.1038/s41467-021-26302-y

Yirmiya, R., Goshen, I., Bajayo, A., Kreisel, T., Feldman, S., Tam, J., Trembovler, V., Csernus, V., Shohami, E., & Bab, I. (2006, Nov 7). Depression induces bone loss through stimulation of the sympathetic nervous system. *Proc Natl Acad Sci U S A, 103*(45), 16876-16881. https://doi.org/10.1073/pnas.0604234103

Żurawek, D., & Turecki, G. (2021). The miRNome of Depression. *International journal of molecular sciences, 22*(21). https://doi.org/10.3390/ijms222111312

7 Article and author information

Jiayao Zhang

Department of Prosthodontics, Stomatological Hospital and Dental School of Tongji University, Shanghai Engineering Research Center of Tooth Restoration and Regeneration, Shanghai, China.

Contribution: Data curation, Investigation, Writing - original draft, Writing - review and editing

For correspondence: michellezhang_07@163.com

Competing interests: No competing interests declared

Juan Li

Department of Prosthodontics, Stomatological Hospital and Dental School of Tongji University, Shanghai Engineering Research Center of Tooth Restoration and Regeneration, Shanghai, China.

Contribution: Data curation, Investigation, Validation; Formal analysis

For correspondence: 15025002369@163.com
Competing interests: No competing interests declared

Jiehong Huang
Department of Neurology and Neurological Rehabilitation, Shanghai Yangzhi Rehabilitation Hospital, School of Medicine, Tongji University, Shanghai, China
Contribution: Methodology; Software; Validation; Formal analysis
For correspondence: jh_huang1996@163.com
Competing interests: No competing interests declared

Xuerui Xiang
Department of Neurology and Neurological Rehabilitation, Shanghai Yangzhi Rehabilitation Hospital, School of Medicine, Tongji University, Shanghai, China
Contribution: Methodology; Software; Validation; Formal analysis
For correspondence: sherry199503@163.com
Competing interests: No competing interests declared

Ruoyu Li
Department of Neurology and Neurological Rehabilitation, Shanghai Yangzhi Rehabilitation Hospital, School of Medicine, Tongji University, Shanghai, China
Contribution: Methodology; Software; Validation; Formal analysis
For correspondence: liry_1996@163.com
Competing interests: No competing interests declared

Yun Zhai
Department of Prosthodontics, Stomatological Hospital and Dental School of Tongji University, Shanghai Engineering Research Center of Tooth Restoration and Regeneration, Shanghai, China.
Contribution: Methodology; Data curation
For correspondence: 904890219@qq.com
Competing interests: No competing interests declared

Shuxian Lin
Department of Prosthodontics, Stomatological Hospital and Dental School of Tongji University, Shanghai Engineering Research Center of Tooth Restoration and Regeneration, Shanghai, China.
Contribution: Conceptualization; Funding acquisition; Supervision; Writing - review and editing
For correspondence: shuxian.lin@hotmail.com
Contributed equally with: Weicai Liu
Competing interests: No competing interests declared

Weicai Liu
Department of Prosthodontics, Stomatological Hospital and Dental School of Tongji

University, Shanghai Engineering Research Center of Tooth Restoration and Regeneration, Shanghai, China.
Contribution: Conceptualization; Funding acquisition; Supervision; Writing - review and editing
For correspondence: vogi@163.com
Contributed equally with: Shuxian Lin
Competing interests: No competing interests declared

8 Funding

National Natural Science Foundation of China (81873709)

- Shuxian Lin

Shanghai Health Committee (20204Y0278)

- Shuxian Lin

National Natural Science Foundation of China (8227032547)

- Weicai Liu

Natural Science Foundation of Shanghai (20ZR1463000)

- Weicai Liu

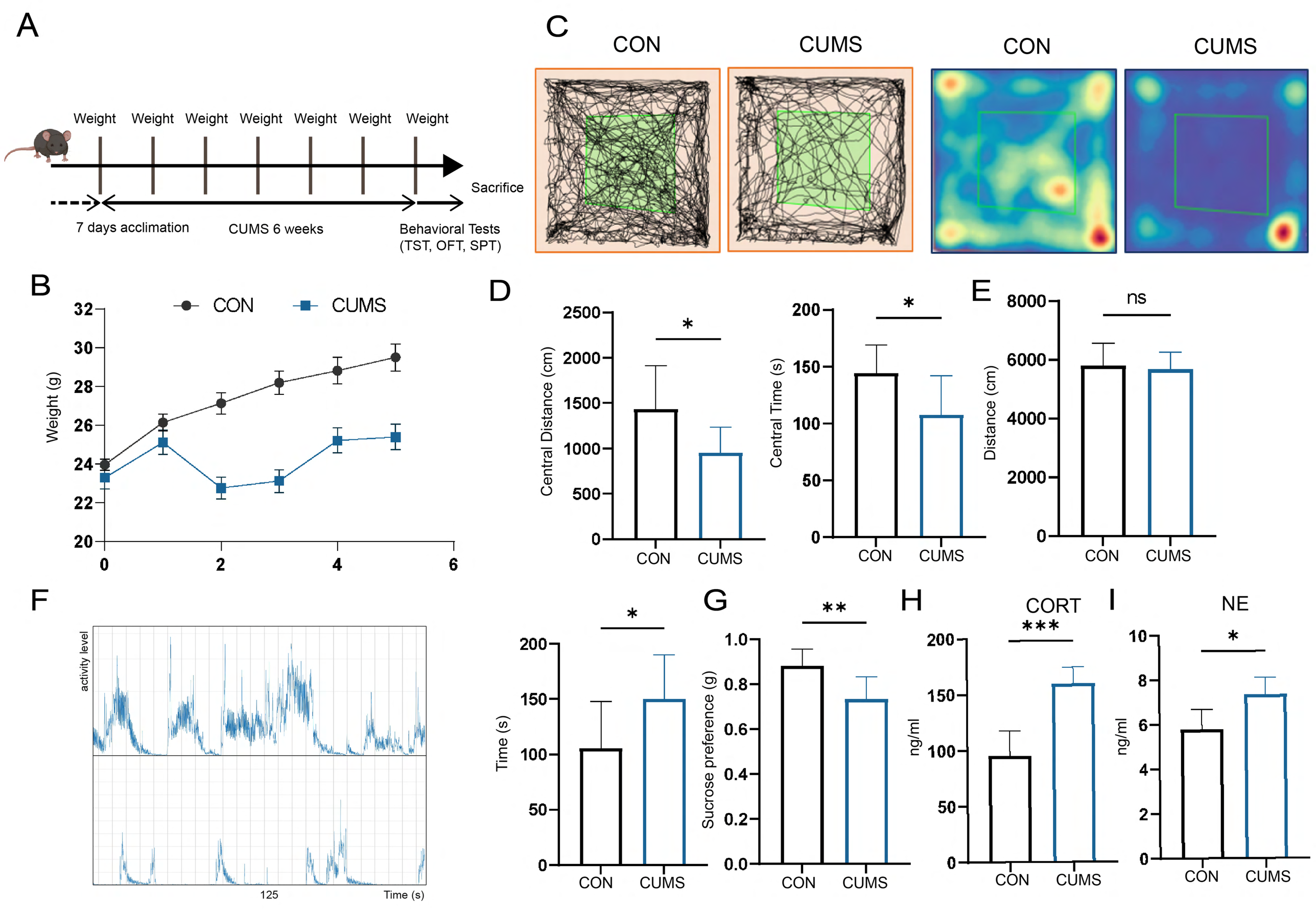
A
Weight
Weight
Weight
Weight
Weight
Weight
Weight
Sacrifice
7 days acclimation
CUMS 6 weeks
Behavioral Tests
(TST, OFT, SPT)
B
CON
CUMS
Weight (g)
32
30
28
26
24
22
20
0
2
4
6
C
CON
CUMS
CON
CUMS
D
Central Distance (cm)
2500
2000
1500
1000
500
0
*
CON
CUMS
Central Time (s)
200
150
100
50
0
*
CON
CUMS
E
Distance (cm)
8000
6000
4000
2000
0
ns
CON
CUMS
F
activity level
125
Time (s)
G
Time (s)
200
150
100
50
0
*
CON
CUMS
Sucrose preference (g)
1.0
0.8
0.6
0.4
0.2
0.0
**
CON
CUMS
H
CORT
ng/ml
200
150
100
50
0
***
CON
CUMS
I
NE
ng/ml
10
8
6
4
2
0
*
CON
CUMS

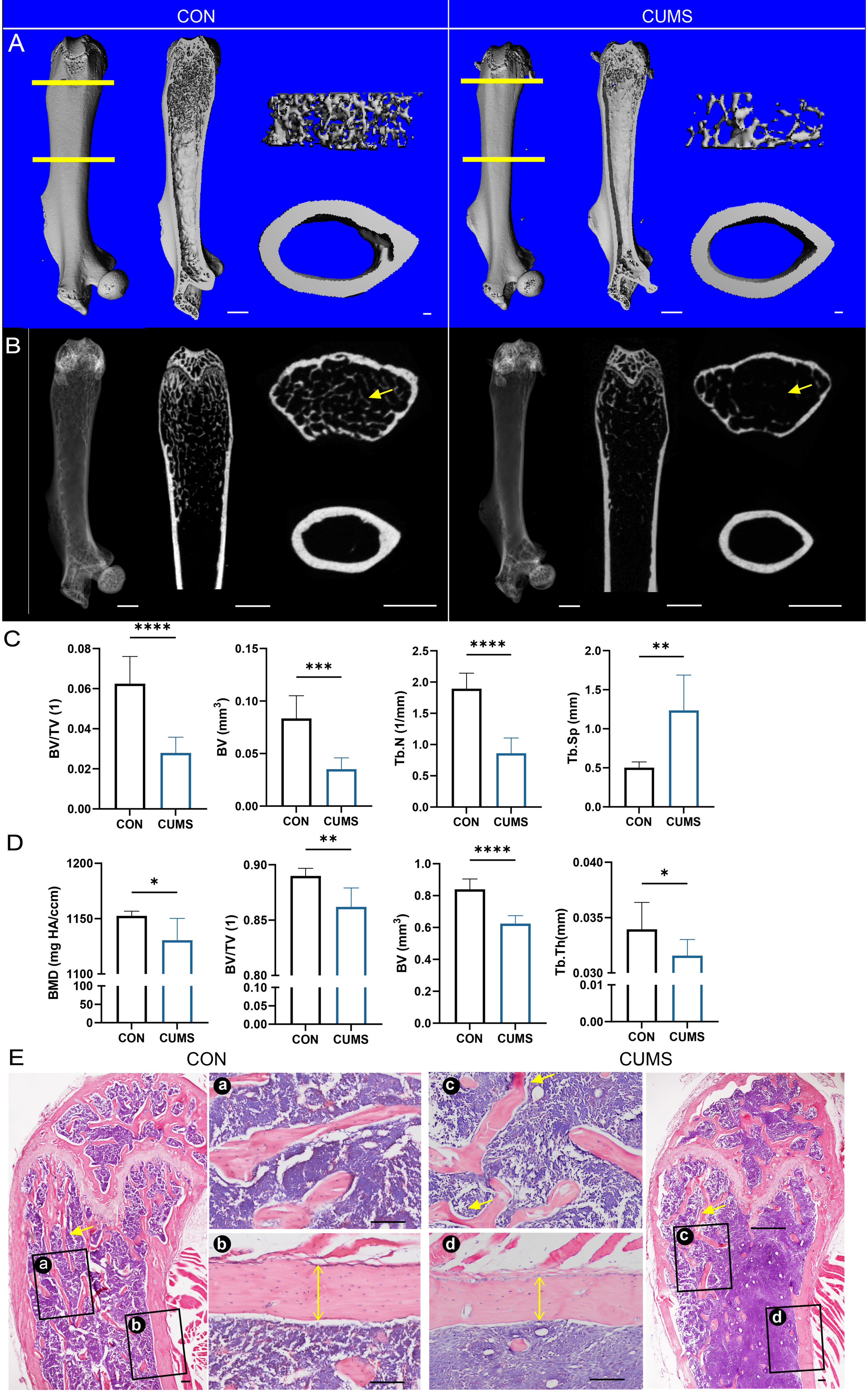
CON
CUMS
A
B
C
BV/TV (1)
BV (mm3)
Tb.N (1/mm)
Tb.Sp (mm)
CON
CUMS
D
BMD (mg HA/ccm)
BV/TV (1)
BV (mm3)
Tb.Th(mm)
E
CON
CUMS
a
b
c
d

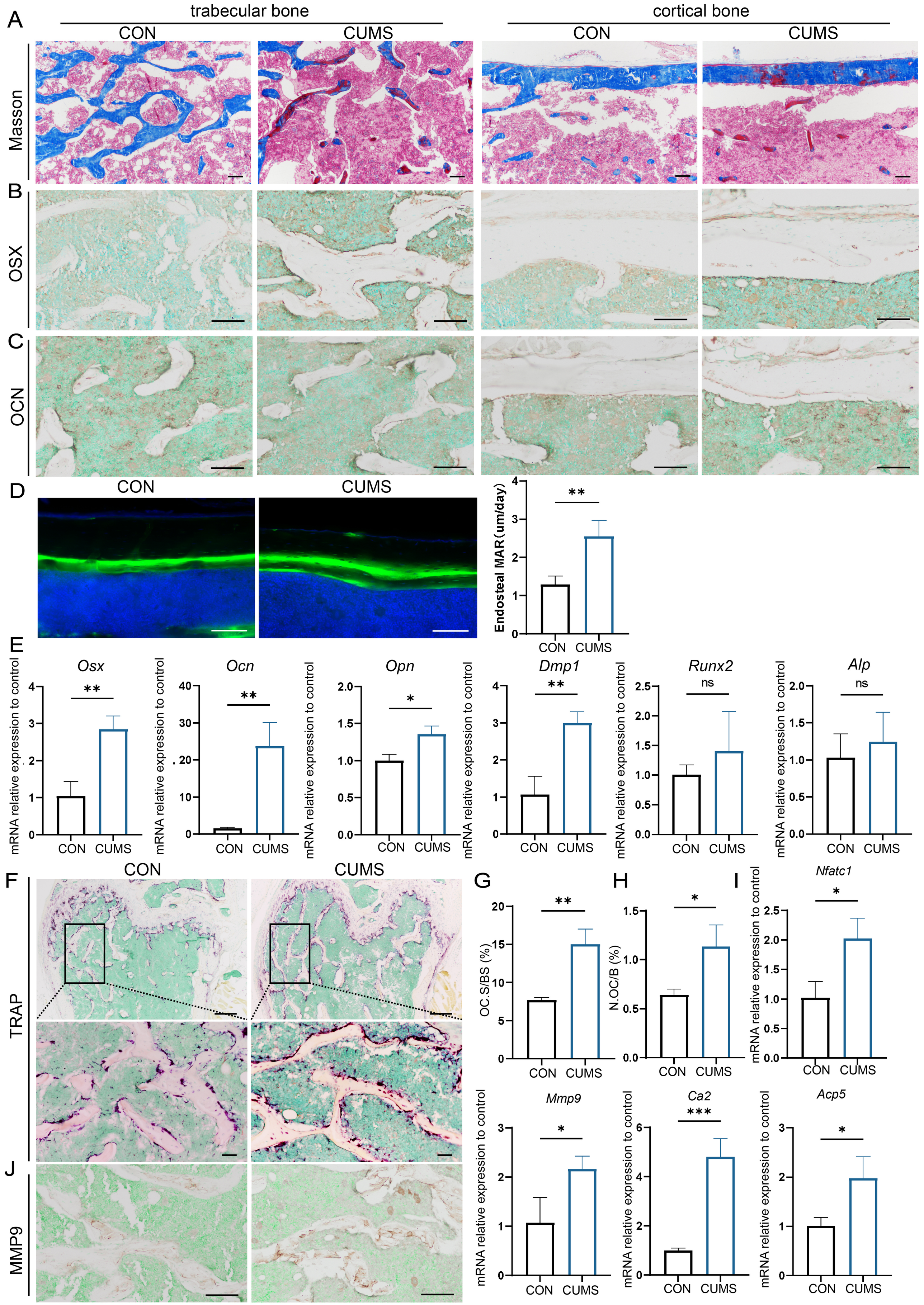
A
trabecular bone
cortical bone
CON
CUMS
CON
CUMS
Masson
B
OSX
C
OCN
D
CON
CUMS
Endosteal MAR（um/day）
**
CON
CUMS
E
Osx
Ocn
Opn
Dmp1
Runx2
Alp
mRNA relative expression to control
**
**
*
**
ns
ns
CON
CUMS
F
CON
CUMS
TRAP
G
OC.S/BS (%)
**
H
N.OC/B (%)
*
I
Nfatc1
*
J
MMP9
Mmp9
*
Ca2
***
Acp5
*

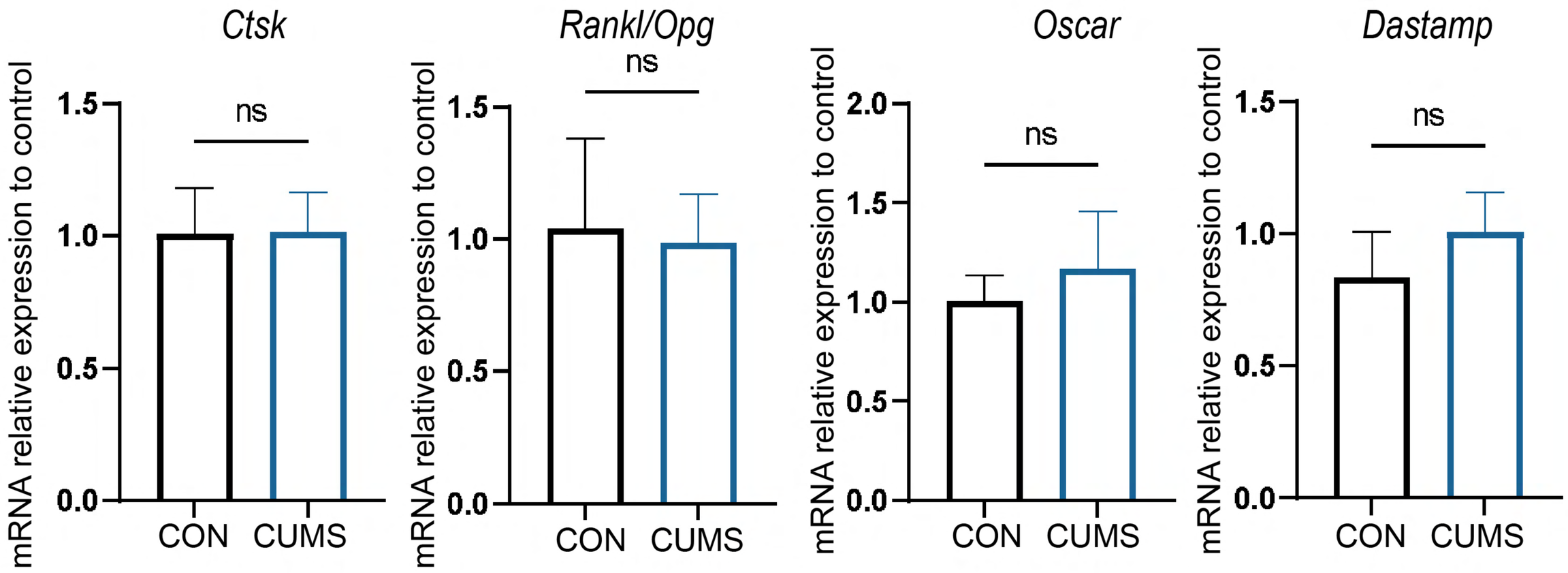
Ctsk
mRNA relative expression to control
1.5
1.0
0.5
0.0
ns
CON
CUMS
Rankl/Opg
mRNA relative expression to control
1.5
1.0
0.5
0.0
ns
CON
CUMS
Oscar
mRNA relative expression to control
2.0
1.5
1.0
0.5
0.0
ns
CON
CUMS
Dastamp
mRNA relative expression to control
1.5
1.0
0.5
0.0
ns
CON
CUMS

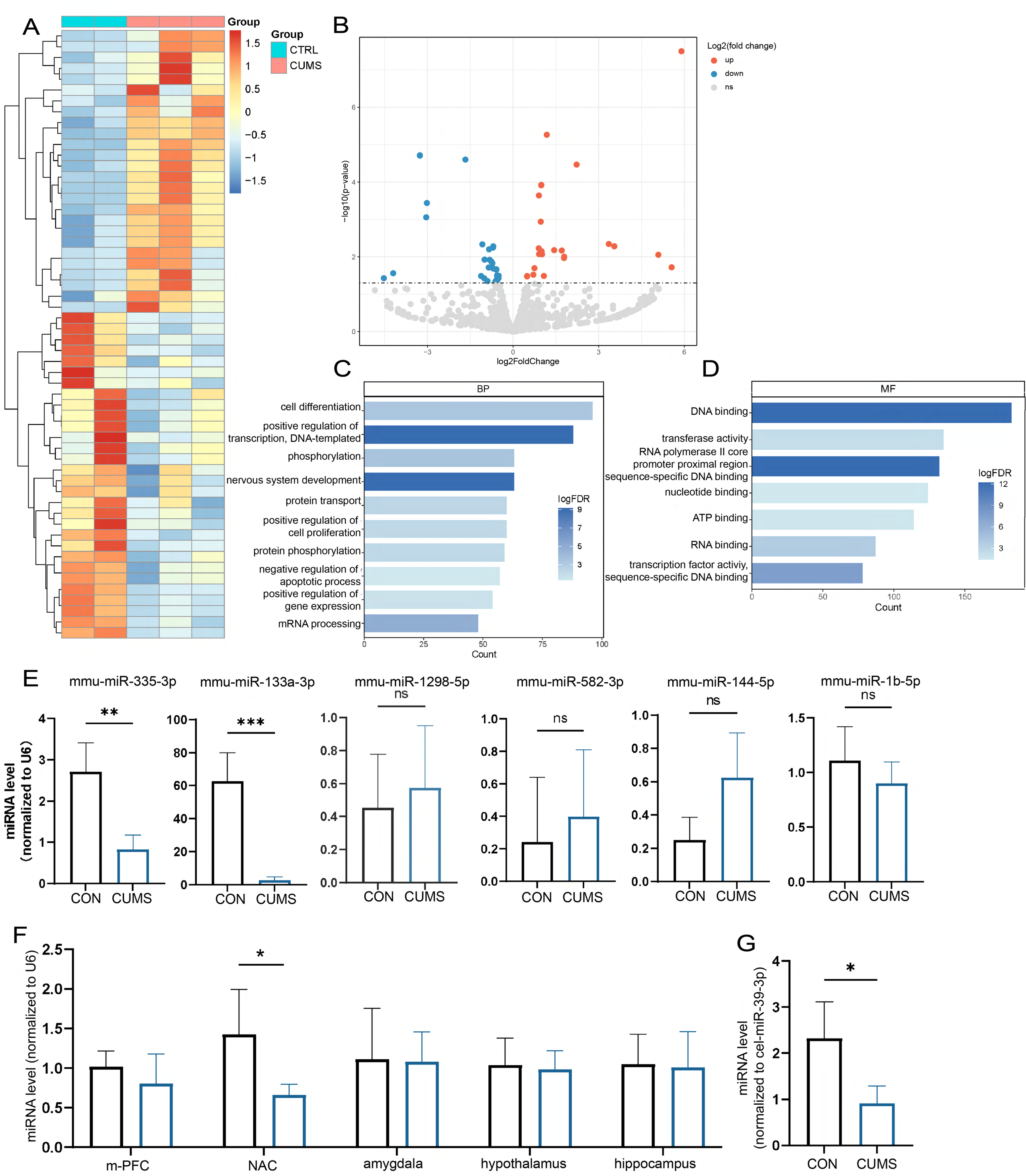
A
Group
CTRL
CUMS
1.5
1
0.5
0
−0.5
−1
−1.5
B
Log2(fold change)
up
down
ns
−log10(p−value)
log2FoldChange
C
BP
cell differentiation
positive regulation of transcription, DNA-templated
phosphorylation
nervous system development
protein transport
positive regulation of cell proliferation
protein phosphorylation
negative regulation of apoptotic process
positive regulation of gene expression
mRNA processing
logFDR
Count
D
MF
DNA binding
transferase activity
RNA polymerase II core promoter proximal region sequence-specific DNA binding
nucleotide binding
ATP binding
RNA binding
transcription factor activiy, sequence-specific DNA binding
logFDR
Count
E
mmu-miR-335-3p
mmu-miR-133a-3p
mmu-miR-1298-5p
mmu-miR-582-3p
mmu-miR-144-5p
mmu-miR-1b-5p
miRNA level (normalized to U6)
CON
CUMS
F
miRNA level (normalized to U6)
m-PFC
NAC
amygdala
hypothalamus
hippocampus
G
miRNA level (normalized to cel-miR-39-3p)
CON
CUMS

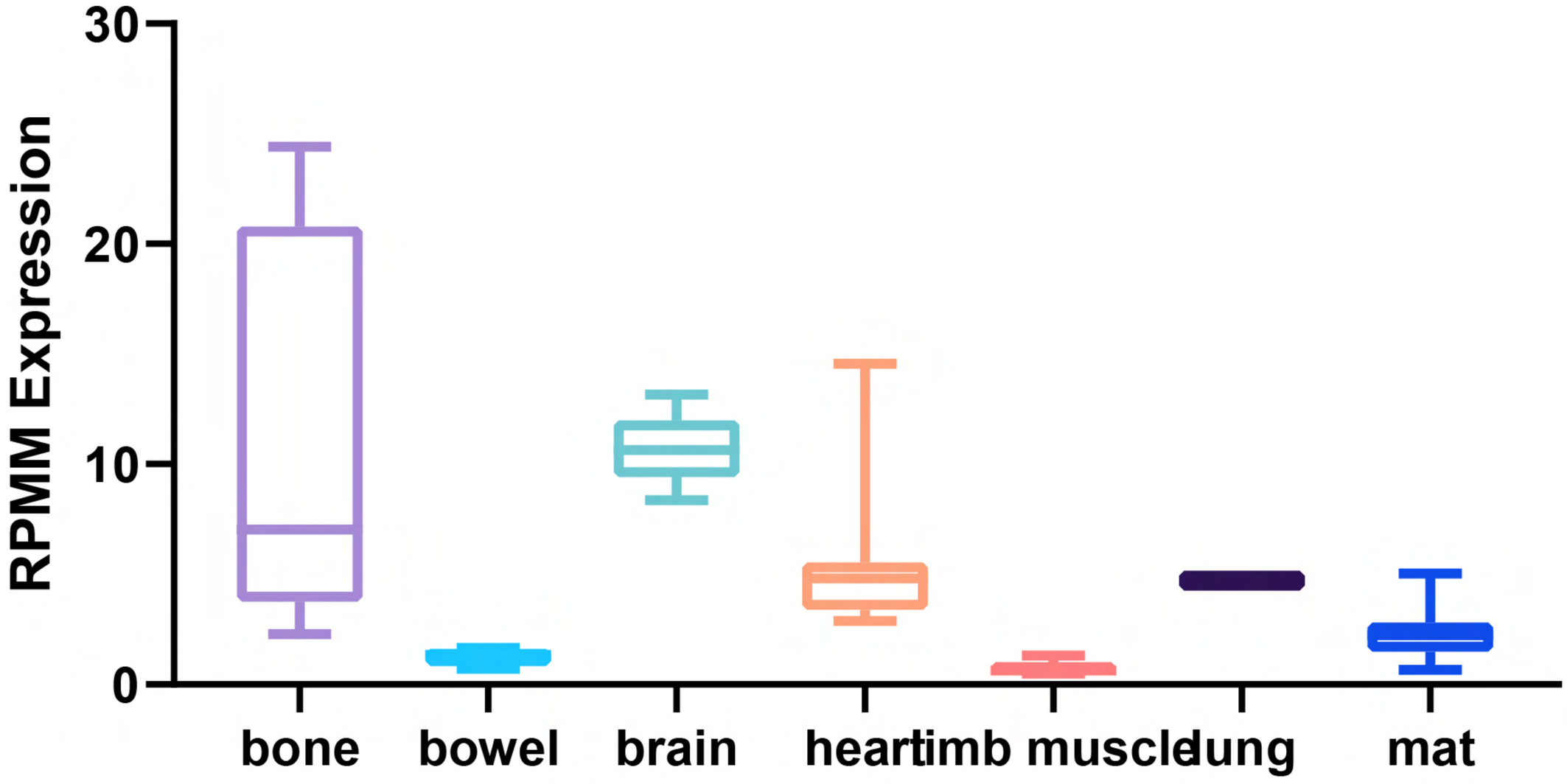
RPMM Expression
30
20
10
0
bone
bowel
brain
heart
timb
muscle
lung
mat

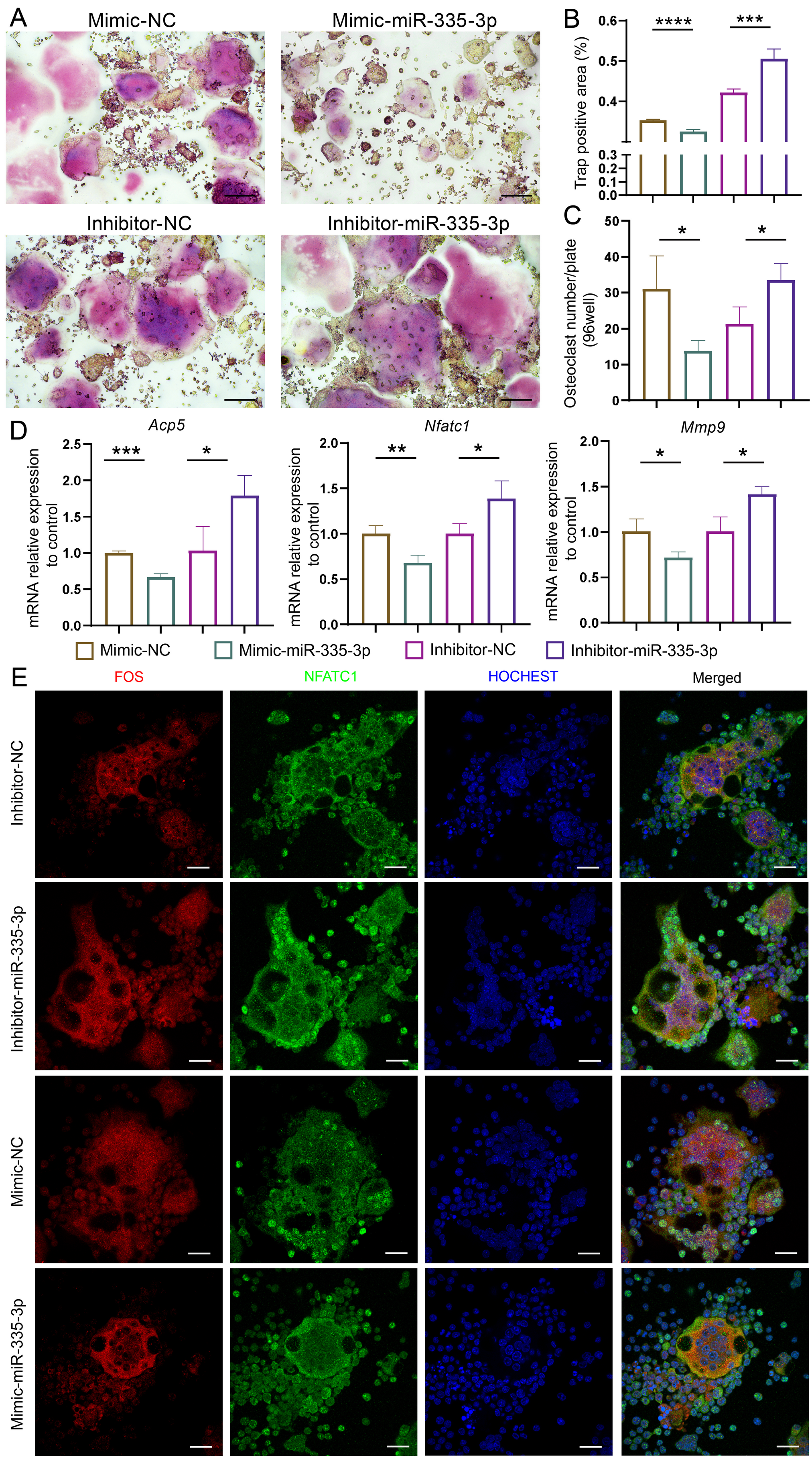
A
Mimic-NC
Mimic-miR-335-3p
Inhibitor-NC
Inhibitor-miR-335-3p
B
Trap positive area (%)
0.6
0.5
0.4
0.3
0.2
0.1
0.0
****
***
C
Osteoclast number/plate (96well)
50
40
30
20
10
0
*
*
D
Acp5
Nfatc1
Mmp9
mRNA relative expression to control
2.5
2.0
1.5
1.0
0.5
0.0
***
*
**
*
*
*
Mimic-NC
Mimic-miR-335-3p
Inhibitor-NC
Inhibitor-miR-335-3p
E
FOS
NFATC1
HOCHEST
Merged
Inhibitor-NC
Inhibitor-miR-335-3p
Mimic-NC
Mimic-miR-335-3p

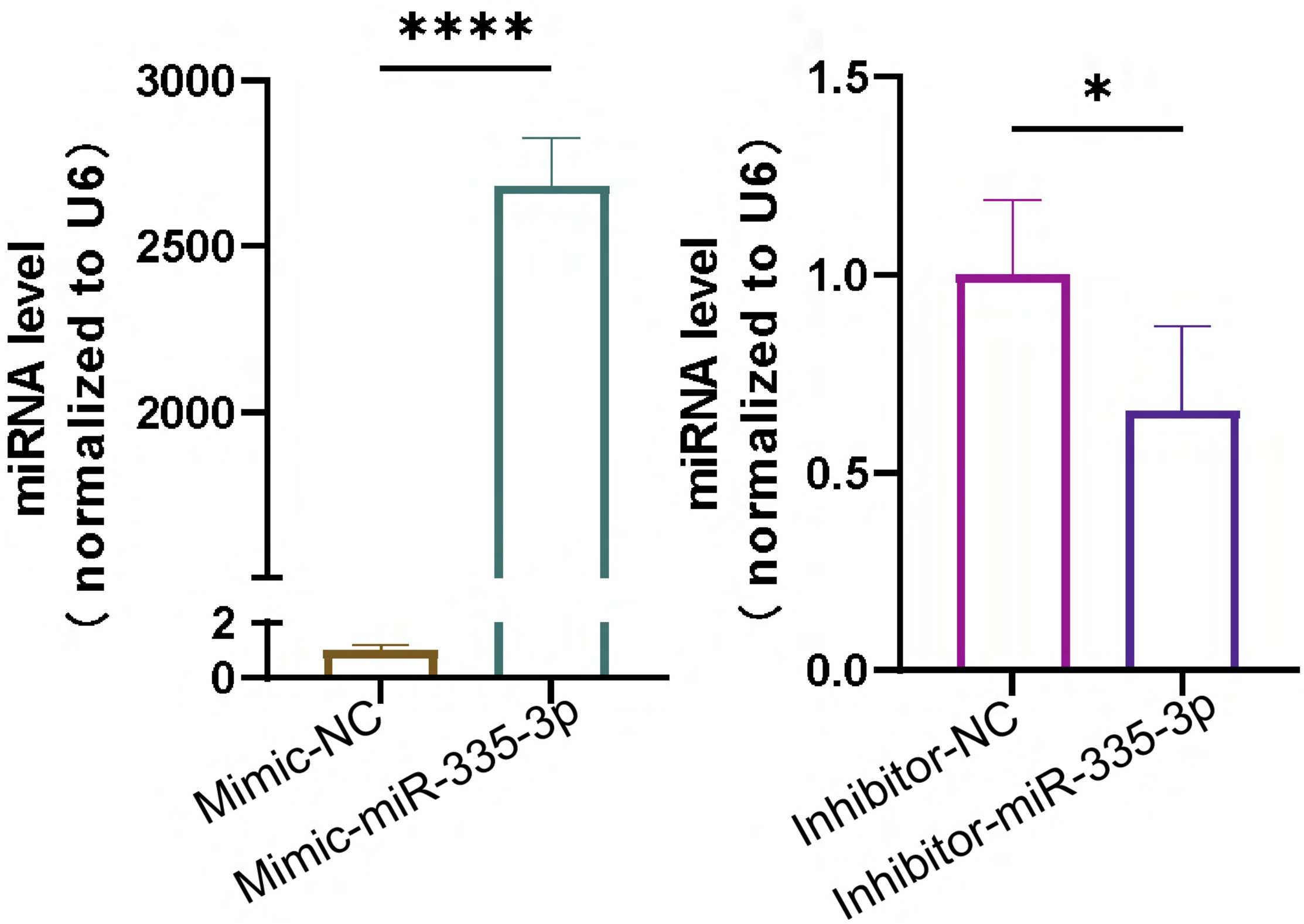
****
3000
2500
2000
2
0
miRNA level
（normalized to U6）
Mimic-NC
Mimic-miR-335-3p
*
1.5
1.0
0.5
0.0
miRNA level
（normalized to U6）
Inhibitor-NC
Inhibitor-miR-335-3p

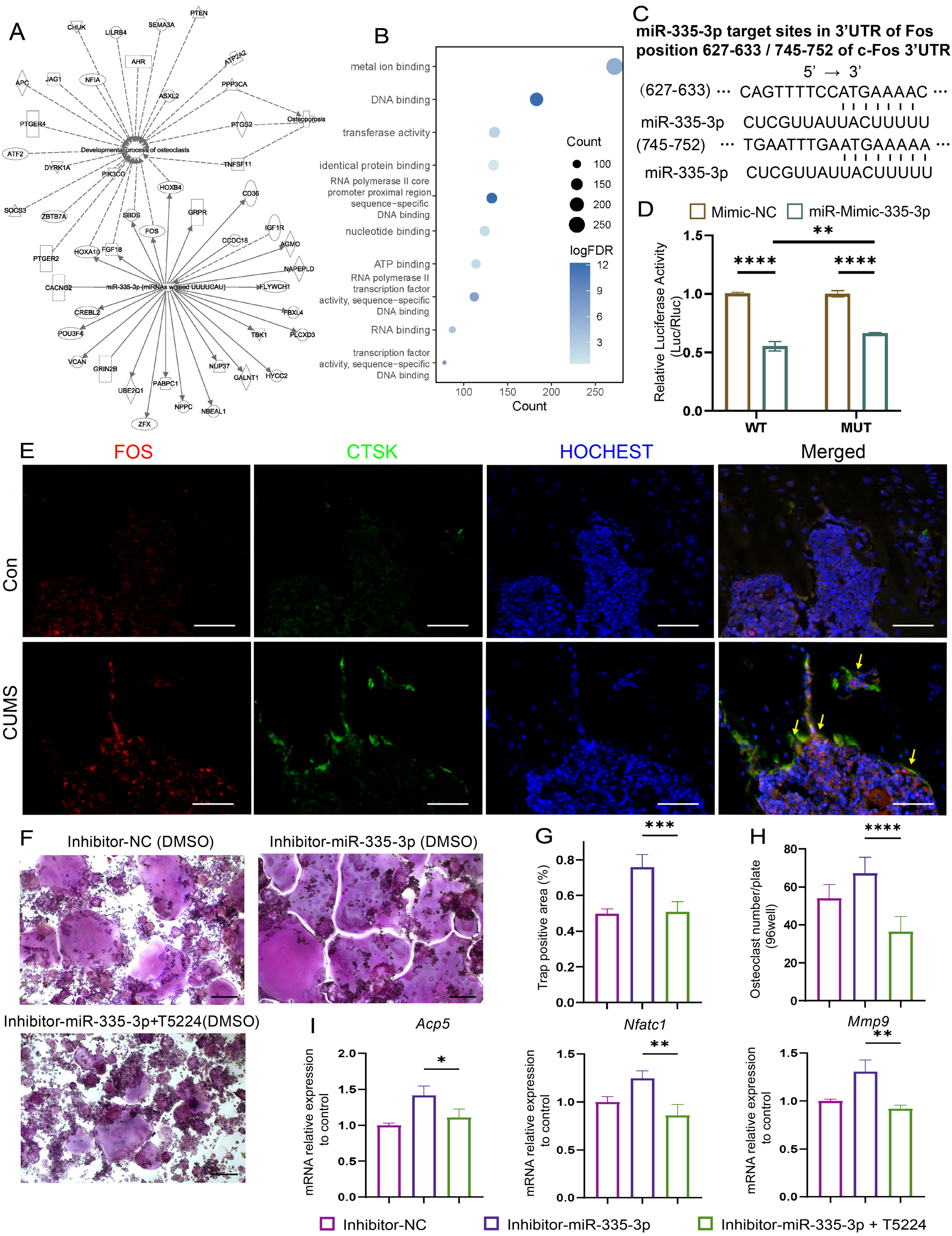
A
PTEN
CHUK
LILRB4
SEMA3A
AHR
ATP2A2
APC
JAG1
NFIA
PPP3CA
ASXL2
PTGER4
PTGS2
Osteoporosis
ATF2
Developmental process of osteoclasts
DYRK1A
TNFSF11
PIK3CG
HOXB4
CD36
SOCS3
ZBTB7A
SBDS
GRPR
FOS
IGF1R
CCDC18
AGMO
HOXA10
FGF18
PTGER2
NAPEPLD
CACNG2
miR-335-3p (miRNAs w/seed UUUUCAU)
FLYWCH1
CREBL2
FBXL4
POU3F4
TBK1
PLCXD3
VCAN
GRIN2B
NUP37
GALNT1
HYCC2
UBE2Q1
PABPC1
NPPC
NBEAL1
ZFX
B
metal ion binding
DNA binding
transferase activity
identical protein binding
RNA polymerase II core promoter proximal region sequence-specific DNA binding
nucleotide binding
ATP binding
RNA polymerase II transcription factor activity, sequence-specific DNA binding
RNA binding
transcription factor activity, sequence-specific DNA binding
100
150
200
250
Count
Count
100
150
200
250
logFDR
12
9
6
3
C
miR-335-3p target sites in 3'UTR of Fos
position 627-633 / 745-752 of c-Fos 3'UTR
5' → 3'
(627-633) ··· CAGTTTTCCATGAAAAC ···
miR-335-3p CUCGUUAUUACUUUUU
(745-752) ··· TGAATTTGAATGAAAAA ···
miR-335-3p CUCGUUAUUACUUUUU
D
Mimic-NC
miR-Mimic-335-3p
Relative Luciferase Activity (Luc/Rluc)
1.5
1.0
0.5
0.0
**
****
****
WT
MUT
E
FOS
CTSK
HOCHEST
Merged
Con
CUMS
F
Inhibitor-NC (DMSO)
Inhibitor-miR-335-3p (DMSO)
Inhibitor-miR-335-3p+T5224(DMSO)
G
***
Trap positive area (%)
0.8
0.6
0.4
0.2
0.0
H
****
Osteoclast number/plate (96well)
80
60
40
20
0
I
Acp5
*
mRNA relative expression to control
2.0
1.5
1.0
0.5
0.0
Nfatc1
**
mRNA relative expression to control
1.5
1.0
0.5
0.0
Mmp9
**
mRNA relative expression to control
1.5
1.0
0.5
0.0
Inhibitor-NC
Inhibitor-miR-335-3p
Inhibitor-miR-335-3p + T5224

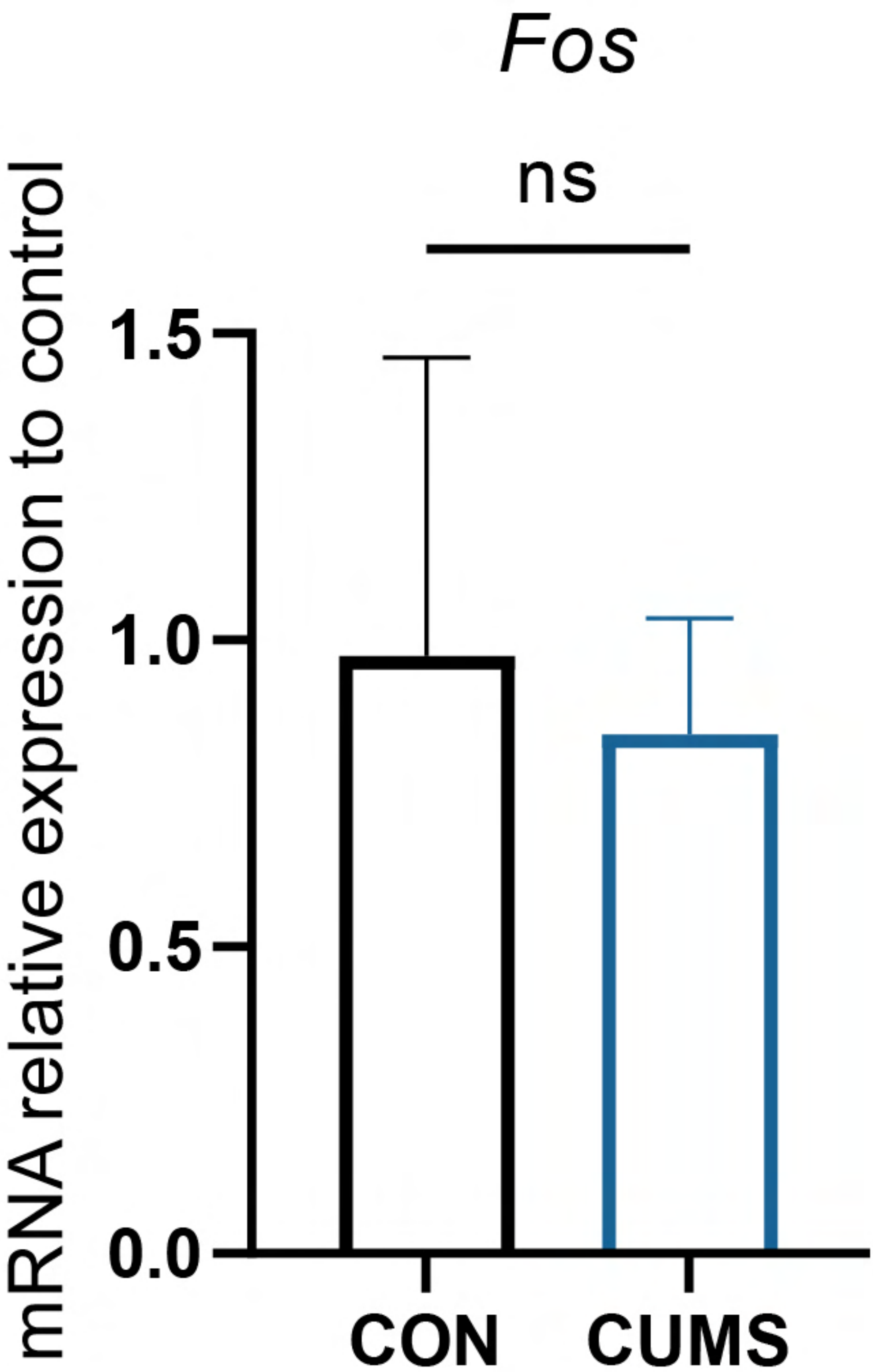
Fos
ns
mRNA relative expression to control
1.5
1.0
0.5
0.0
CON
CUMS

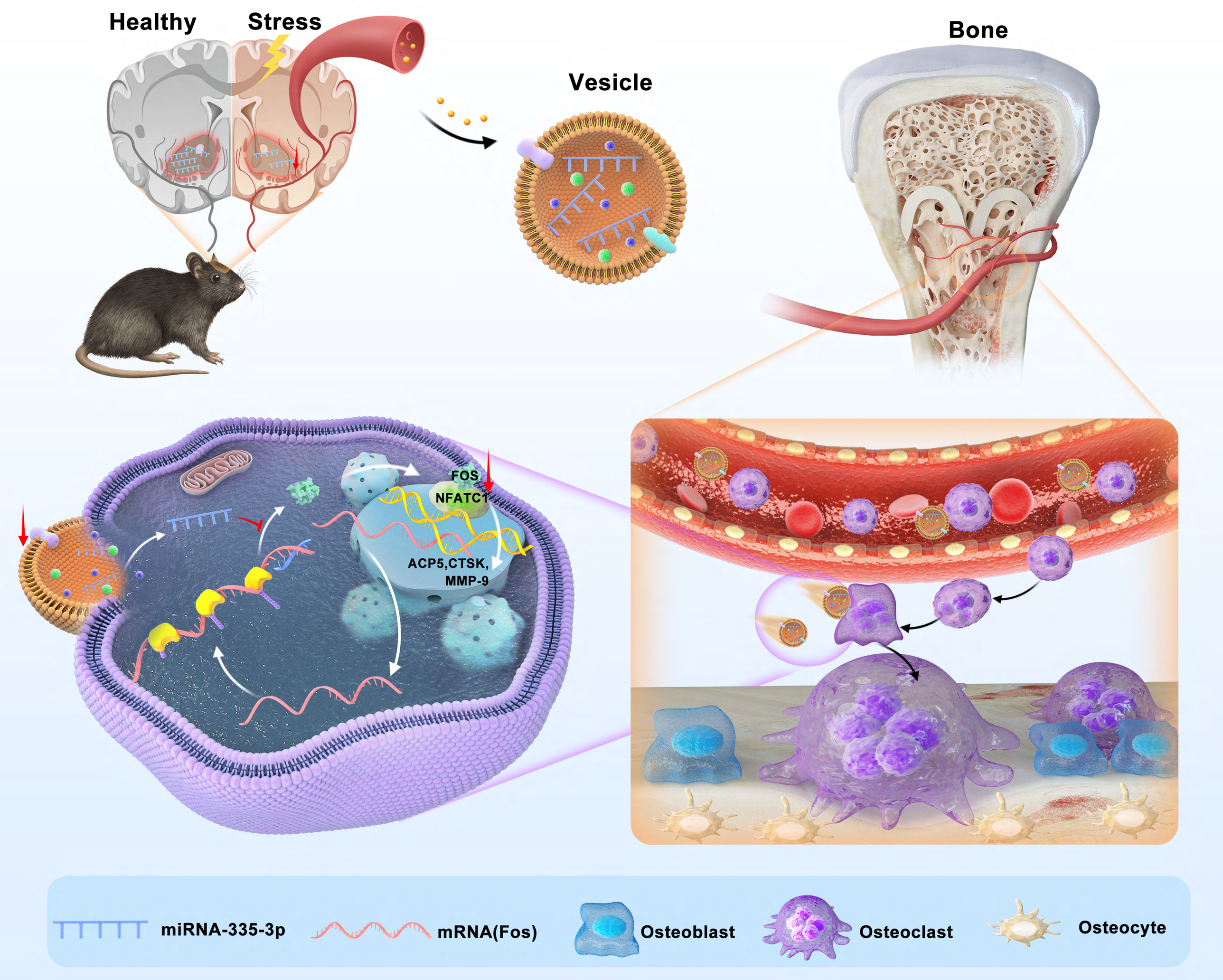
Healthy
Stress
Vesicle
Bone
FOS
NFATC1
ACP5,CTSK,
MMP-9
miRNA-335-3p
mRNA(Fos)
Osteoblast
Osteoclast
Osteocyte